0026-895X/01/6004-797–807$3.00
MOLECULAR PHARMACOLOGY
Copyright © 2001 The American Society for Pharmacology and Experimental Therapeutics
Mol Pharmacol 60:797–807, 2001

Vol. 60, No. 4
966/931955
Printed in U.S.A.

The Kinetics of Competitive Antagonism by Cisatracurium of Embryonic and Adult Nicotinic Acetylcholine Receptors

DEEPTANKAR DEMAZUMDER and JAMES P. DILGER

Department of Physiology and Biophysics, State University of New York (SUNY) at Stony Brook, and Department of Anesthesiology, Health Sciences Center at SUNY Stony Brook, Stony Brook, New York

Received March 13, 2001; accepted July 3, 2001

This paper is available online at http://molpharm.aspetjournals.org

ABSTRACT

Competitive antagonists to nicotinic acetylcholine receptors are clinically used as muscle relaxants. Previously, we reported the kinetics of inhibition (in the absence of acetylcholine) by (+)-tubocurarine and pancuronium on embryonic receptors. Here, we examine cisatracurium, a commonly used muscle relaxant. Outside-out patches were equilibrated with cisatracurium before application of 300 μM acetylcholine. cisatracurium inhibited the initial peak current, but the decay of these currents displayed a pronounced biphasic behavior. The IC_{50} value was 54 $\pm$ 2 nM and 115 $\pm$ 4 nM for adult and embryonic receptors, respectively. We designed a rapid perfusion system to apply or remove cisatracurium for various times before application of acetylcholine. We determined the association (embryonic, 3.4 $\pm$ 0.4 $\times$ 10^8 M^{-1} s^{-1}; adult, 1.8 $\pm$ 0.3 $\times$ 10^8 M^{-1} s^{-1}) and dissociation (embryonic, 34 $\pm$ 6/s; adult: 13 $\pm$ 5/s) rates for cisatracurium. Association was 2.9- and 1.3-fold greater than that of (+)-tubocurarine and pancuronium, respectively. Dissociation was 6- and 16-fold higher than (+)-tubocurarine and pancuronium, respectively. These measurements correspond to dissociation of cisatracurium from receptors in the absence of acetylcholine. Physiologically, acetylcholine interacts with receptors equilibrated with antagonist. We developed a mathematical technique that removes the effect of desensitization and determined dissociation (embryonic, 52 $\pm$ 9/s; adult, 33 $\pm$ 5/s) in the presence of acetylcholine. These data suggest that presence of acetylcholine on one binding site of the receptor increases the dissociation rate of antagonist from the other binding site. We incorporated all of these rates into a computer simulation of a comprehensive 11-state Markov model. There was excellent agreement (without curve fitting) between simulated and experimental currents.

The nicotinic acetylcholine receptor (nAChR), found on neurons in the central and peripheral nervous system and muscle cells at the neuromuscular junction, is the prototypical ionotropic ligand-gated ion channel (Dilger, 1997). There are two isoforms of muscle-type nAChR. The embryonic isoform differs from the adult by one subunit (γ instead of ϵ) of five and has a conductance of 40 pS (in the adult, 60 pS) and a mean open-time three times longer than in the adult isoform. Muscles that are not innervated (i.e., during development) express only embryonic nAChR that are uniformly distributed at moderate density in the synapse. During innervation, the embryonic isoform is replaced by the adult isoform at the synapse; the embryonic isoform is still present but aggregates around the periphery of the synapse.

Functionally, rapid synaptic transmission is achieved partly because nAChR is a single protein containing both the ligand-receptor and ion-channel. Action potentials propagate in the presynaptic nerve terminal, and ACh is exocytosed into the synapse. ACh diffuses across the synaptic cleft (~0.2 ms) and binds to sites on muscle-type nAChR at the α-δ (high-affinity) and α-γ (low-affinity) subunit interfaces. The channels open for an average of 1 ms and allow the entry of sodium ions that depolarize the postsynaptic terminal. Under normal circumstances, the depolarization reaches threshold and the muscle fiber fires an action potential that results in muscle contraction. After the channel closes, ACh dissociates and is hydrolyzed within ~0.2 ms by acetylcholinesterase; the entire synaptic event is complete within a few milliseconds. The continued presence of ACh induces nAChR to enter a nonconducting conformation, or desensitization, with a higher affinity for ACh.

Competitive antagonists to nAChR are clinically used to immobilize patients during surgery. Several studies have shown they have a higher affinity (as much as 100-fold) for α-γ/ϵ site compared with the α-δ site (Arias, 2000; Fletcher and Steinbach, 1996). They have little or no efficacy for channel gating, and the occupancy of only one site is necessary to prevent normal activation by ACh. The binding affinities for several antagonists have been measured, including

This research was supported in part by a grant from the National Institute of General Medical Sciences (GM42095), and the Department of Anesthesiology, State University of New York at Stony Brook. These data were presented at the 44th and 45th Annual Meetings of Biophysical Society: *Biophys J* **78:**359, 2000; *Biophys J* **80:**463, 2001; and *Biophys J* **80:**462, 2001.

ABBREVIATIONS: nAChR, nicotinic acetylcholine receptor; ACh, acetylcholine; cisatr, cisatracurium; HEK, human embryonic kidney; ECS, extracellular solution; mAChR, muscarinic acetylcholine receptor; OD, desensitized state; O, open state.

(+)-tubocurarine, the prototypical antagonist. Several studies attempted to determine the kinetics of inhibition for (+)-tubocurarine but there was little agreement among their findings (Colquhoun and Sheridan, 1982; Le Dain et al., 1991; Aoshima et al., 1992; Bufler et al., 1996). This controversy was recently re-examined in experiments from our laboratory (Wenningmann and Dilger, 2001).

From a physiological point of view, determining the association and dissociation rate constants of competitive antagonists is important because the free concentration of ACh and the degree of ACh occupancy on the receptors do not reach equilibrium during a synaptic event. Moreover, the rates may provide insight into the clinical effects of competitive antagonists. For example, it may be possible for an antagonist with a high dissociation rate to dissociate from nAChR during a synaptic event, thereby allowing ACh to activate these receptors. Such an antagonist would probably have a lower clinical potency (compared with an antagonist with a lower dissociation rate). It might also have a faster clinical onset of action because its diffusion will be buffered to a lesser extent by the embryonic (extrajunctional) receptors (Glavinovic et al., 1993). Finally, these rates are necessary for the incorporation of antagonists into any model of the neuromuscular junction.

Here, we examined the kinetics of competitive antagonism by cisatracurium (cisatr), a commonly-used muscle relaxant with a clinical potency 10-fold greater than that of (+)-tubocurarine (Savarese et al., 2000). We made electrophysiological measurements from outside-out patches containing embryonic or adult wild-type nAChR. In equilibrium experiments, the patch was preincubated with cisatr before application of 300 μM ACh. Interestingly, the decay of these currents displayed a biphasic behavior (secondary increase in current at high concentrations of cisatr). This biphasic behavior was also observed for (+)-tubocurarine, albeit to a lesser extent (Wenningmann and Dilger, 2001), and it was predicted by others (Aoshima et al., 1992). To further investigate this phenomenon, we developed a rapid perfusion system allowing measurement of the degree of nAChR inhibition after brief exposure (< 1 ms) or washout of antagonist. With this system, we determined the association and dissociation rate constants for cisatr. These measurements correspond to the kinetics of cisatr antagonism in the absence of ACh. During a synaptic event, ACh interacts with receptors equilibrated with antagonist. To investigate this condition, we developed a technique that reveals the time course of dissociation of antagonist in the presence of ACh. We incorporated all of these rates into a computer simulation of a comprehensive 11-state Markov model that describes competitive antagonism of cisatr on embryonic and adult nAChR.

Materials and Methods

General Methods. Clonal BC_3H1 cells that express mouse embryonic ($\alpha_2\beta\gamma\delta$) nAChR (Schubert et al., 1974) were cultured as described previously (Sine and Steinbach, 1984). HEK-293 cells were transfected with the calcium-phosphate precipitation method to express adult ($\alpha_2\beta\epsilon\delta$) nAChR (Prince and Sine, 1996). At the time of electrophysiological experiment, the culture medium was replaced with extracellular solution (ECS) and patch electrodes were filled with intracellular solution, as described in Wenningmann and Dilger (2001). The three-tube perfusion system used here (Fig. 1) differs from that of Wenningmann and Dilger (2001) in that the minimum solution exposure time was 0.5 rather than 10 ms. The improvement in time resolution was due to a steeper angle and better alignment between tubes, and uniform high-precision orifice edges that produced a more laminar flow.

The currents were measured with a patch clamp amplifier (EPC-9; List Electronic, Darmstadt, Germany), sampled at 50 μs per point, filtered at 6.7 kHz, digitized and stored on the hard disk drive of a laboratory computer (Pentium II 266 MHz, 20 GB hard disk drive). Data were analyzed with routines (specifically written for each protocol) in WaveMetrics Igor Pro macro language and imported into Microsoft Excel for presentation purposes. All data values are expressed as mean ± S.D.

Equilibrium Measurements. The outside-out patch was voltage-clamped at −50 or + 50 mV. Only two tubes were used for these experiments. For the control series, the patch was equilibrated with ECS for at least 5 s, and then perfused with ECS + ACh for 200 ms. For the drug series, the patch was equilibrated with ECS + cisatr for at least 5 s and then perfused with ECS + cisatr + ACh for 200 ms. These procedures were performed at least 10 times per series per drug concentration per patch. Control series were performed before and after all other series on each patch. Data were accepted only when the recovery was >95%. The ensemble mean current for each series was calculated from the 10 or more individual current traces.

For control series, the decay of the mean current after the rapid onset was fit to a one-exponential function: $I(t) = I_\infty + I_1 \exp(-t/\tau_1)$, τ_1 ranging from 20 to 85 ms. For drug series, a one- or two-exponential function: $I(t) = I_\infty + I_1 \exp(-t/\tau_1) + I_2 \exp(-t/\tau_2)$ was used to fit the mean current decay because the current traces displayed a biphasic behavior in the presence of high cisatr concentrations. The peak current of the rapid onset phase reflects the number of channels that were not inhibited by cisatr during the 5-s exposure to ECS + cisatr, assuming there was no dissociation of cisatr during the onset phase; this assumption was justified by results from the kinetic measurements. The ratio of this current to the peak current from control series (I_{DRUG}/I_0) represents the fractional inhibition of nAChR by cisatr. The fractional inhibition values for all patches were plotted as a function of cisatr concentration and the data were fit to the Hill and two-site binding model equations [see equations 1 and 2 in Wenningmann and Dilger (2001)]. Comparison between two data sets was performed by fitting the Hill and two-site binding model equations to the fractional inhibition data for each patch, and the mean IC_{50}, L_1, and L_2 values were tested for statistical significance using an unpaired two-tailed t test.

Measurement of Cisatr Kinetics in the Absence of ACh. All three tubes were used for "onset" and "recovery" protocols. The

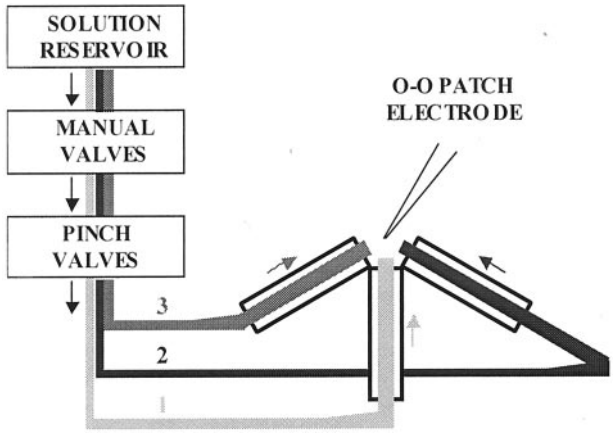

Fig. 1. Schematic of the 3-tube rapid perfusion system. The pinch valves controlled the flow of solution through the tubes such that only one solution was flowing to the patch at any time. The perfusion system allowed rapid solution exchange (0.1–0.2 ms) between tubes and a minimum solution exposure time of 0.5 ms. Only two tubes were used for the equilibrium measurements.

outside-out patch was voltage-clamped at −50 or + 50 mV. For the onset protocol, the patch was equilibrated with ECS for at least 5 s from tube 1, then perfused with ECS + cisatr for varying intervals of time (0–600 ms) from tube 2, and finally perfused with ECS + cisatr + ACh for 200 ms from tube 3. For the recovery protocol, the patch was equilibrated with ECS + cisatr for at least 5 s from tube 1, then perfused with ECS for varying intervals of time (0–600 ms) from tube 2, and finally perfused with ECS + ACh for 200 ms from tube 3. These procedures were performed for 20 different time intervals per protocol. Each protocol was repeated at least five times at each concentration of cisatr per patch (n = 3 per concentration per protocol). A control series was also performed before and after each onset and recovery protocol and data were accepted only when the recovery was >95%. At the end of each experiment, the patch was blown off the electrode and solution exposure times were ascertained by using the onset and recovery protocols on the open-electrode using solutions with different NaCl concentrations. The data analysis was similar to equilibrium experiments. Fractional inhibition was plotted as a function of cisatr exposure or washout time for onset and recovery protocols, respectively. The data were fit to a one-exponential function.

We often observed a marked, albeit inconsistent, slowing of the onset and recovery kinetics for cisatr on patches from the HEK-293 cells transfected with the adult receptor. For example, in the recovery protocol, even after 600 ms of washout of cisatr (concentrations ranging from 50 to 3000 nM), the peak currents were only 80 ± 18% (n = 19; ranging from 24 to 100%) of control values. In contrast, after 300 ms of washout of cisatr from patches from BC_3H1 cells, peak currents were 101 ± 5% (n = 15) of control values. We observed the same phenomenon when we transfected the HEK-293 cells with embryonic nAChR, suggesting that it is specific for this cell line. We considered the possibility that the HEK-293 cells contain an endogenous binding site for cisatr. Endogenous muscarinic acetylcholine receptors (mAChR) have been reported in intact HEK-293 cells using a radiolabeled binding assay with N-[^{3}H]methylscopolamine (Zhu et al., 1998). To our knowledge, the binding affinity of cisatr for mAChR has not been measured. An in vivo study in cats has reported that high concentrations of cisatr inhibit the response to vagal (parasympathetic) nerve stimulation (Wastila et al., 1996). Moreover, recent studies using radiolabeled binding assays have shown that several competitive antagonists to nAChR (including (+)-tubocurarine) bind to mAChR with affinities in the micromolar range (Waelbroeck, 1994; Hou et al., 1998). More specifically, the binding affinity of atracurium [consisting of 15% cisatr in a mixture of nine other isomers (Savarese et al., 2000)] for the M_2 and M_3 subtypes of mAChR was determined to be 5 and 1.4 μM, respectively (Hou et al., 1998). Based on these findings, we hypothesized that the diffusion of cisatr was buffered by the endogenous mAChR expressed in HEK-293 cells, thereby affecting our kinetic measurements in the onset and recovery protocols. Subsequently, we added 1 μM atropine (mAChR antagonist) to our solutions and the currents recovered to 101 ± 4% (n = 12) of control values within 600 ms of washout of cisatr from patches from HEK-293 cells with adult receptors. We note that 1 μM atropine was used in another study to isolate neuronal nAChR from mAChR currents in HEK-293 cells (Buisson and Bertrand, 1998). This concentration of atropine did not affect the peak amplitude or time course of the currents from our control and drug series. Thus, we conclude that cisatr inhibition of nAChR is not sensitive to 1 μM atropine, consistent with the binding affinity of 150 μM measured for atropine on embryonic nAChR (Amitai et al., 1987). All data reported here for adult receptors were obtained in the presence of 1 μM atropine.

Measurement of Cisatr Kinetics in the Presence of ACh. In the control series, the decay of the ensemble mean current after the rapid onset was fit to a one-exponential function: $I(t) = I_\infty + I_1 \exp(-t/\tau_1)$; the onset ($k_{+D}$) and recovery ($k_{-D}$) rates of desensitization were determined from the fit, assuming a simple two-state model (open state or desensitized state), using the following two equations:

$$\tau_1 = \frac{1}{k_{+D} + k_{-D}} \quad (1a)$$

$$\frac{I_\infty}{I_0} = \frac{k_{-D}}{k_{+D} + k_{-D}} \quad (1b)$$

Data were collected using a two-tube perfusion protocol (similar to that in the drug series) in which the patch was equilibrated with ECS + cisatr (25, 50, 150, 300, 900, or 3000 nM) for at least 5 s, and then perfused with ECS + ACh. Using numerical analysis, we calculated (time step = 50 μs; Δt) the fraction of receptors in the desensitized state (OD) as a function of time (t):

$$OD(t) = OD(t - \Delta t) + O(t - \Delta t) \times k_{+D} \times \Delta t - OD(t - \Delta t) \times k_{-D} \times \Delta t \quad (2)$$

By adding the fraction of receptors in the open state (O) to OD, we removed the effects of desensitization with the assumption that the rates of desensitization are not affected by cisatr. Because activation of receptors by 300 μM ACh is rapid, the rate-limiting step is the dissociation of cisatr. Thus, the result of O + OD represents the apparent time course of cisatr dissociation. By fitting O + OD to a one-exponential function, the time constant revealed the dissociation rate constant in the presence of ACh (ℓ'_{-1}; see Fig. 2). We divided this rate by the IC_{50} value (determined from equilibrium experiments) to calculate the association rate constant in the presence of ACh (ℓ'_{+1}). The kinetics of cisatr measured with the O + OD technique from adult receptors were not changed by the presence of 1 μM atropine. Here, we report the combined data collected in the absence and presence of 1 μM atropine.

Measurement of Hetero-Liganded Openings at Low Concentrations of ACh. We measured single channel currents from

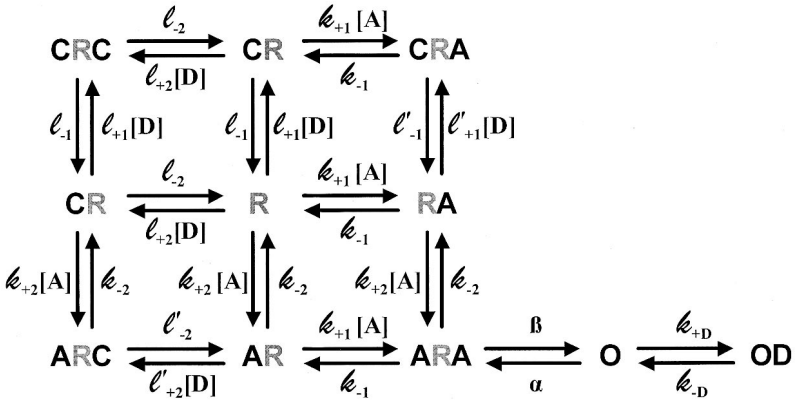

Fig. 2. 11-state model. The model assumes there are two distinct binding sites for agonist (low-affinity, **A**R; high-affinity, R**A**) and competitive antagonists (low-affinity, R**C**; high-affinity, **C**R), no single-liganded or hetero-liganded openings, and that the channel opens (O) before it desensitizes (OD). Rate constants for cisatr in the absence (ℓ_{+1} and ℓ_{-1}) and presence (ℓ'_{+1} and ℓ'_{-1}) of ACh were determined for the high-affinity binding site in this study. We tested several values for rates of the low affinity site (ℓ_{+2}, ℓ_{-2}, ℓ'_{+2}, and ℓ'_{-2}) consistent with the difference in affinity between the two binding sites (see *Results*). We used rate constants published previously (Zhang et al., 1995; Auerbach and Akk, 1998) for ACh binding (k_{+1}, k_{-1}, k_{+2}, and k_{-2}) and gating (β and α). Rate-constants for desensitization (k_{+D} and k_{-D}) were calculated for each patch.

embryonic receptors with 200 nM ACh in the absence or presence of 300 nM cisatr. We calculated the number of openings and the mean open and shut times using the SCAN software (http://www.ucl.ac.uk/Pharmacology/dcpr95.html). We also measured current responses to 1 μM ACh with various concentrations of cisatr and calculated the ensemble mean average. We modified the 11-state model (Fig. 2) to incorporate a hetero-liganded open state (one-ACh-bound + one-antagonist-bound open state, where both ligands are bound to their high affinity site; CRA in Fig. 2), and simulated currents with 1 μM ACh. We varied the hetero-liganded opening rate until the simulation matched experimental responses.

Computer Simulation. Experimental currents were simulated using Euler's method of numerical integration on a set of equations from an 11-state model (Fig. 2). The model assumes there are two distinct binding sites for agonist (low-affinity, **A**R; high-affinity, R**A**) and competitive antagonists (low-affinity, R**C**; high-affinity, **C**R), no single-liganded or hetero-liganded openings, and that the channel opens (O) before it desensitizes (OD). The entire model consisted of 10 differential equations and an additional one-exponential equation describing the time course of solution exchange. Some simulations were performed assuming a single hetero-liganded open state from CRA in Fig. 2. Rate constants for cisatr in the absence (ℓ_{+1} and ℓ_{-1}) and presence (ℓ'_{+1} and ℓ'_{-1}) of ACh were determined for the high-affinity binding site in the previous sections. We tested several values for rates of the low-affinity site (ℓ_{+2}, ℓ_{-2}, ℓ'_{+2}, and ℓ'_{-2}), consistent with the difference in affinity between the two binding sites determined from equilibrium measurements. We used rate constants published previously (Zhang et al., 1995; Auerbach and Akk, 1998) for ACh binding (k_{+1}, k_{-1}, k_{+2}, and k_{-2}) and gating (β and α). Rate constants for desensitization (k_{+D} and k_{-D}) were calculated for each patch as described in the previous section. Solution of the model involved specifying initial steady-state conditions (R, CR, RC, CRC; calculated using the two-site binding model equation) for the differential equations, with subsequent integration of the equations as a function of time.

The consistency of the relationship between currents generated by the 11-state model simulation and those measured experimentally was assessed using R^2, the coefficient of determination:

$$R^2 = 1 - \frac{\sum [\text{Simulated Data} - \text{Experimental Data}]^2}{\sum [\text{Experimental Data} - \text{Mean (Experimental Data for all time points)}]^2} \quad (3)$$

The "goodness of fit" between a current measured experimentally and currents generated by the 11-state model simulation with varying parameters was assessed using a χ^2 method:

$$\chi^2 = \sum [\text{Simulated Data} - \text{Experimental Data}]^2 \quad (4)$$

A lower χ^2 value denotes a better fit. Differences between χ^2 values were assessed for statistical significance using a variance ratio test (Zar, 1999).

Results

Equilibrium Measurements. Representative traces from control and drug series on embryonic receptors are shown in Fig. 3. For the control series, exposure to 300 μM ACh produced a rapid onset and the peak current represents approximately 95% open channels (Dilger and Brett, 1990). The current decays with a time constant of approximately 30 ms as receptors desensitize in the continued presence of ACh. For the drug series, the patch was equilibrated with ECS + cisatr, and perfused with ECS + cisatr + ACh for 200 ms. The peak current of the rapid onset phase represents channels activated by ACh within 100 to 200 μs. The peak current is reduced with increasing cisatr concentrations (as expected for a competitive antagonist) because cisatr occupies the ACh-binding site on nAChR and prevents activation by ACh. However, at high cisatr concentrations (>50 nM), the currents display a biphasic time course (after the rapid onset). This biphasic behavior becomes more pronounced with increasing concentrations of cisatr.

The fractional inhibition (mean ± S.D. for each cisatr concentration) of embryonic and adult receptors is plotted as a function of cisatr concentration in Fig. 4. The original data (before averaging for each concentration) were fit to the Hill and two-site binding model equations; the results are listed in Table 1. The IC_{50} value was similar to L_1 for both embryonic and adult receptors. The IC_{50} (115 ± 4 nM) and L_1 (120 ± 6 nM) values for embryonic receptors are not voltage dependent and are 2-fold larger than those for adult receptors. The L_2 values were 33-, 17- and 8-fold greater than those of L_1 for embryonic (−50 mV), embryonic (+50 mV), and adult receptors, respectively. The significantly ($p < 0.0001$) larger S.D. values of L_2 compared with L_1 were related to the lower precision of the data at higher cisatr concentrations.

Measurement of cisatr Kinetics Using Onset and Recovery Protocols. The three-tube perfusion system (Fig. 1) was used to measure the kinetics of embryonic and adult nAChR inhibition by cisatr. Results from a typical onset protocol using 300 nM cisatr on embryonic receptors are shown in Fig. 5. With increasing exposure times, the peak current of the rapid onset phase is reduced and the rest of the current trace manifests a biphasic behavior. Even after only 1.4 ms of exposure time, cisatr has occupied a significant fraction of nAChR such that the current is reduced by 15%. The I_{DRUG}/I_0 values were plotted as a function of cisatr exposure time and fit to a one-exponential function. The recovery protocol was similar to the onset protocol; the patch was equilibrated with ECS + cisatr, then cisatr was washed-off with ECS for various intervals of time (0–600 ms), then the patch was perfused with ECS + ACh for 200 ms. Figure 6 shows an example of an exposure-response curve from onset and recovery protocols using 300 nM cisatr on embryonic receptors. The values of ℓ_{+1} and ℓ_{-1} were determined by fitting each exposure-response curve to a one-exponential function, assuming a single (high-affinity) site binding model (Fletcher and Steinbach, 1996):

$$\text{CR} \underset{\ell_{-1}}{\overset{\ell_{+1} \times [\text{DRUG}]}{\rightleftharpoons}} \text{C} + \text{R} \quad (5)$$

Because ACh is not present, there are no open channels. The time constant of the one-exponential function is given by:

$$\tau = \frac{1}{\ell_{+1} \times [\text{DRUG}] + \ell_{-1}} \quad (6)$$

Plots of the reciprocal of the time constant versus cisatr concentrations from onset and recovery protocols in embryonic and adult receptors are shown in Fig. 7. The slope of the plot from onset protocols represents ℓ_{+1}, and the ordinate-intercept represents ℓ_{-1}. A more precise estimate of ℓ_{-1} was obtained (average of all points) from the recovery protocol, and this result was consistent with the ℓ_{-1} measured independently from the onset protocol. The values of ℓ_{-1} and ℓ_{+1} were tested for statistical significance between adult and embryonic receptors using an unpaired,

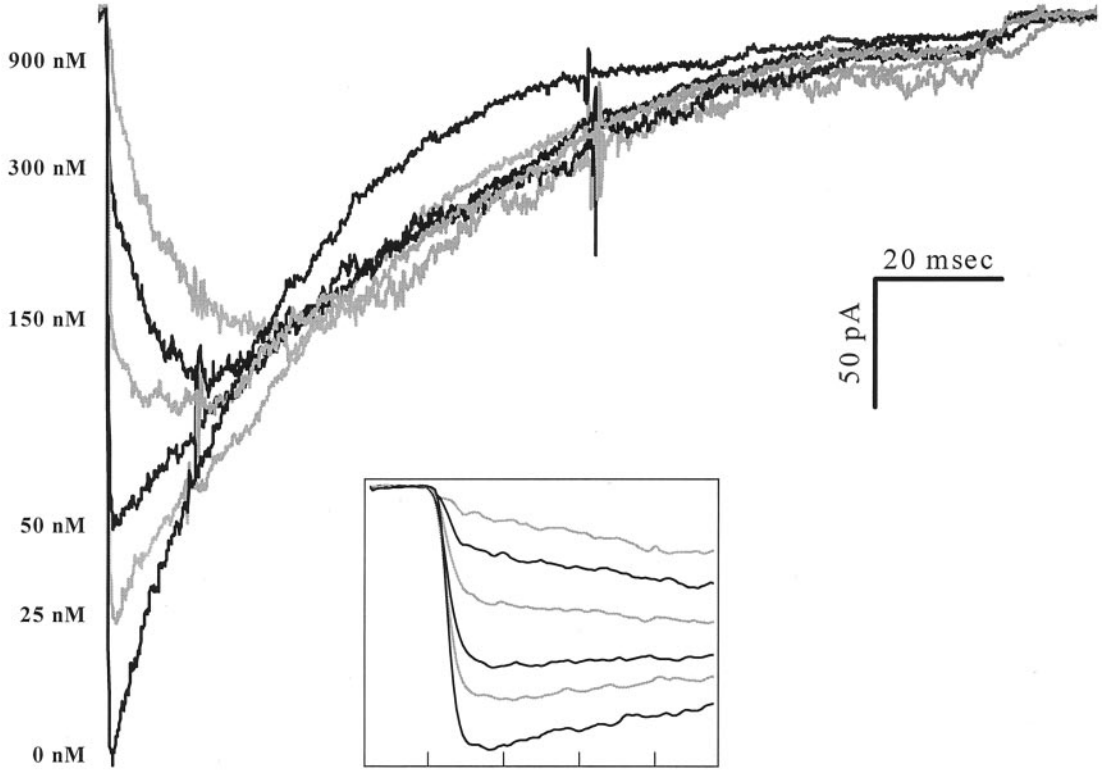

Fig. 3. Representative traces (alternating black and gray) from control and drug series on embryonic receptors at −50 mV. For the control series (0 nM), exposure to 300 μM ACh produced a rapid onset and the current decays with a time constant of approximately 30 ms as the receptors desensitize in the continued presence of ACh. For the drug series, the patch was equilibrated with cisatr, and perfused with cisatr + ACh for 200 ms. The peak current of the rapid onset phase represents channels activated by ACh within 100 to 200 μs. The corresponding cisatr concentrations for each drug series is labeled at the peak of the rapid onset. The peak current is reduced with increasing cisatr concentrations. At high cisatr concentrations (>50 nM), the currents display a biphasic time course (after the rapid onset). This biphasic behavior becomes more pronounced with increasing concentrations of cisatr. Current jumps seen at 15 and 60 ms are artifacts caused by activation/deactivation of the solenoid-driven pinch valves. The inset displays the traces at a higher time resolution (1-ms separation between tick marks).

two-tailed t test. The results are listed in Table 2. In embryonic receptors, ℓ_{-1} was not significantly different at V = +50 and −50 mV and was 3-fold greater than that for adult receptors. The ℓ_{+1} value of embryonic receptors was 2-fold greater than that of adult receptors. For both adult and embryonic receptors, ℓ_{-1}/ℓ_{+1} was not significantly

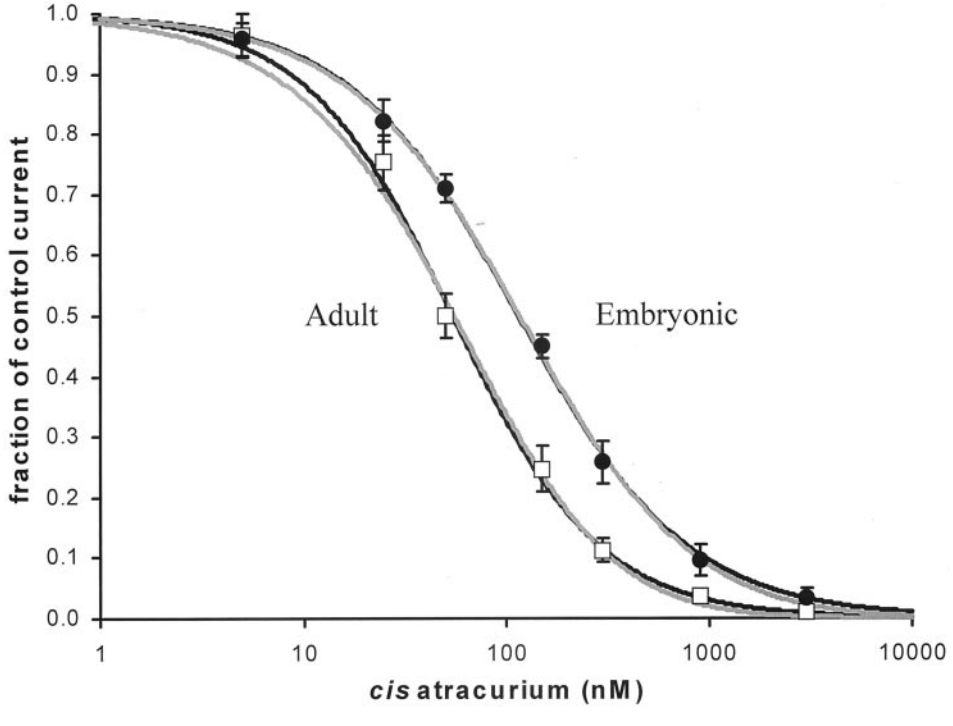

Fig. 4. Concentration-response curve for embryonic (●) and adult (□) receptors at −50 mV. The ratio of the peak current from drug series to that from control series represents the fractional inhibition of nAChR by cisatr. They were fit to the Hill equation (black line) and 2-site binding model (gray line); the fitting parameters are given in Table 1.

different from the IC_{50} value (Welch-corrected unpaired, two-tailed t test).

Measurement of cisatr Kinetics in the Presence of ACh Using Numerical Analysis. In the absence of desensitization, it would be relatively easy to determine the dissociation rate of a competitive antagonist in the presence of ACh. If the patch is equilibrated with ECS + cisatr, and then perfused with ECS + ACh, there will be a rapid onset (representing activation by ACh of nAChR not occupied by cisatr) followed by a secondary increase in current on a slower time scale (representing activation by ACh as cisatr dissociates from nAChR). This slower second component would increase until all cisatr molecules had dissociated from nAChR and the current reached the same steady-state level as control. The time constant of an exponential fit to the second component would represent the dissociation rate constant. The fast time course of desensitization precludes such a simple measurement. It should be possible, however, to remove the effects of desensitization and extract the kinetic information from experimental data.

A two-tube perfusion protocol was used to equilibrate the patch with cisatr and then simultaneously (within 200 μs) remove cisatr and activate channels with ACh. An example with 300 nM cisatr is shown in Fig. 8b. We transformed the current using numerical integration (see *Materials and Methods*) to calculate the time course of the sum of the number of open and desensitized channels (O + OD). We fit O + OD to a one-exponential function and the reciprocal of the time constant revealed ℓ'_{-1}, the dissociation rate constant for cisatr in the presence of ACh. The value of ℓ'_{-1} was tested for statistical significance between embryonic and adult receptors and compared with the corresponding ℓ_{-1} (dissociation rate constant in the absence of ACh) from embryonic and adult receptors using an unpaired, two-tailed t test. The results are listed in Table 2. The value of ℓ'_{-1} was 2.6- and 1.5-fold greater than that of ℓ_{-1} for adult and embryonic receptors, respectively. The value of ℓ'_{-1} for embryonic receptors was 1.6-fold higher than that of adult receptors.

We also calculated O + OD for control currents (Fig. 8a); these yielded a linear horizontal trace (with negligible slope) after the peak rapid onset, suggesting that before desensitizing, most channels are in the open state at 300 μM ACh.

Another two-tube perfusion protocol was used in which the patch was equilibrated with ECS and then perfused with ECS + cisatr + ACh. The peak amplitude and time course of the currents (including rates of desensitization) were the same as control, suggesting that cisatr does not produce any noncompetitive effects at the concentrations used in our study.

Measurement of Hetero-Liganded Openings at Low Concentrations of ACh. Several competitive antagonists, including atracurium, activate a one-ACh-bound + one-antagonist-bound (hetero-liganded) open state in embryonic receptors (Fletcher and Steinbach, 1996). To determine whether this is also true for cisatr, we performed single-channel experiments at low concentrations of ACh. cisatr did not activate any channels by itself. There were fewer openings (65 ± 8% of control; $n = 3$) with 0.2 μM ACh and 300 nM cisatr than with 0.2 μM ACh alone. However, based on macroscopic current measurements with 300 μM ACh and 300 nM cisatr ($n = 4$), we expected the number of openings to be 26 ± 3.5% of control. The greater number of openings at 0.2 μM ACh suggested the activation of a hetero-liganded open state. Consistent with the number of openings, the mean shut time was 2-fold greater in the absence than in the presence of cisatr. The mean open time (~2 ms) was similar under both conditions, suggesting that the closing rate of the hetero-liganded open state was ~500/s. Next, we measured currents at 1 μM ACh with various concentrations of cisatr. Again, there was less inhibition by cisatr than predicted by the IC_{50} value. By comparing these currents with simulated currents using a 12-state model (Fig. 2 with a second open state from CRA), we estimated the hetero-liganded opening rate to be ~25/s. The efficacy of cisatr hetero-liganded openings (25/s / 500/s = 0.05) is similar to that reported for atracurium (Fletcher and Steinbach, 1996).

Computer Simulation. The purpose of performing computer simulations using the 11-state model was to try to reproduce the experimental results, using rate constants for cisatr determined in the previous sections, without implementing any optimization or curve-fitting routines. We used rate constants published previously for ACh binding and gating for embryonic (Zhang et al., 1995) and adult receptors (Auerbach and Akk, 1998). Rate constants for desensitization were determined for each patch; the values of k_{+D} and k_{-D} ranged from 65 to 10/s and 5.5 to 0.064/s, respectively. First, we examined the agreement between experimental currents from equilibrium measurements and simulated currents using the mean values of the rates determined experimentally. The simulated currents accurately reproduced the peak amplitude and time course of experimental currents (R^2 ranging from 0.95 to 1.00). The results of six representative simulations compared with experimental data from the same patch containing embryonic receptors are illustrated in Fig. 9. The agreement between simulated and experimental currents deteriorated with an increase in cisatr concentration. This slight deterioration in R^2 may be attributable, in part, to the smaller (noisier) currents at high cisatr concentrations. The agreement could be further improved by varying ℓ_{-1} or ℓ'_{-1}

TABLE 1

Results of fitting the Equilibrium concentration-response curves (Fig. 4) to the Hill and two-site binding equations [see Wenningmann and Dilger (2001)]

The total number of drug series (n) data for adult, embryonic (−50 mV), and embryonic (+50 mV) receptors were collected from 20, 6, and 11 patches, respectively. Best fit values are given as mean ± S.D. The IC_{50}, L_1, and L_2 values of data from embryonic receptors (−50 mV) were tested for statistical significance (see *Materials and Methods*) with the corresponding data from adult and embryonic (+50 mV) receptors. Values for adult receptors were significantly smaller than those for embryonic receptors (*$p < 0.001$). Values for embryonic receptors were not significantly different at −50 and +50 mV.

nAChR Isoform	n	mV	IC_{50}	Hill Coefficient	L_1	L_2
			nM		*nM*	*nM*
Adult	39	−50	54 ± 2*	1.19 ± 0.04	62 ± 4*	480 ± 180*
Embryonic	22	−50	115 ± 4	1.04 ± 0.04	120 ± 6	4000 ± 3500
Embryonic	23	+50	96 ± 5	1.06 ± 0.05	103 ± 7	1800 ± 1400

around the mean measured value, but without exceeding 1 S.D.

Next, we examined the contribution of some states and kinetic components to the overall shape of the current. For example, we could not directly measure ℓ'_{+1} and the kinetics of cisatr binding to the low-affinity site. Even when we increased or decreased ℓ'_{+1} by 4-fold, the simulation was not sensitive to this parameter. However, the time course of the simulated currents deviated from experimental currents when the $L_2 < 10 \cdot L_1$, suggesting that there is at least a 10-fold difference in affinity between the two cisatr binding sites. Because our calculation of ℓ_{+1} and ℓ_{-1} assumed a single (high-affinity) site binding model (eq. 5), we simulated onset and recovery protocols and varied the dissociation rates for the two sites from unity to a 1000-fold difference. The kinetics measured from the simulated currents were not sensitive to the difference in binding affinity between the two sites and whether the low-affinity site had a slower association or faster dissociation rate. In addition, the simulation was not sensitive to whether or not the high-affinity binding site for ACh and cisatr were the same. To determine the validity of the O + OD technique, we performed simulations using different values for ℓ'_{-1} and ℓ_{-1} and calculated O + OD for the simulated currents. By fitting O + OD to a one-exponential function, the reciprocal of the time constant was equal to the ℓ'_{-1} that we used to simulate the currents. We also performed simulations by modifying the 11-state model to incorporate the hetero-liganded open state. This increased the simulated currents by 6% or less and, in some cases, improved the agreement with experimental data from embryonic receptors.

Finally, we investigated the different roles of ℓ_{-1} and ℓ'_{-1} by comparing our previous results with simulations using $\ell_{-1} = \ell'_{-1}$ or $\ell'_{-1} = \ell_{-1}$. The accuracy of the simulated currents deteriorated at high cisatr concentrations, suggesting that a distinct difference in the rates (ℓ_{-1} and ℓ'_{-1}) is necessary to accurately describe the experimental currents. A comparison at 900 nM cisatr is shown with adult receptors in Fig. 10. In this example, the simulation using ℓ_{-1} and ℓ'_{-1} produced a current-trace that matched the experimental current significantly better than the simulation using $\ell'_{-1} = \ell_{-1}$.

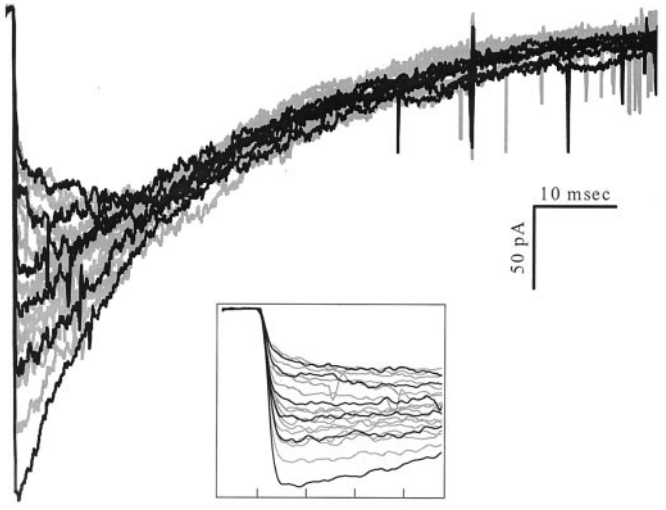

Fig. 5. Results from a representative onset protocol using 300 nM cisatr on embryonic nAChR at −50 mV. The cisatr exposure times were: **0,** 1.4, 2.2, 2.4, **3.0**, 3.2, 3.5, 4.3, **4.6**, 5.1, 5.9, 6.7, **7.7**, 9.1, 10.4, 12.8, **15.4**, 18.8, 23.5, 30.0, and **37.7** ms. The bold-faced exposure times correspond to the black traces. With increasing exposure times, the peak current of the rapid onset phase is reduced and the rest of the current trace manifests a biphasic behavior. The inset displays the traces at a higher time resolution (1-ms separation between tick marks).

Discussion

cisatr is one (*R-cis*, *R′-cis*) of a mixture of 10 isomers that constitutes atracurium. Fletcher and Steinbach (1996), using radiolabeled binding experiments, predicted the IC_{50} value of atracurium to be 270 and 135 nM for embryonic and adult receptors, respectively. Consistent with their findings, we found that the IC_{50} value of cisatr for embryonic receptors is

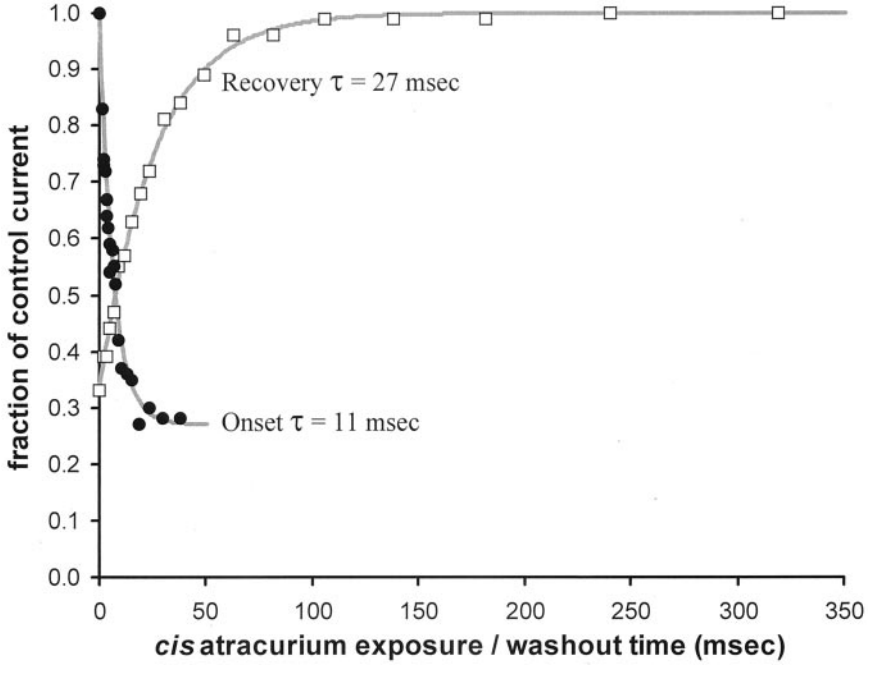

Fig. 6. Exposure-response curves for onset (●, data from Fig. 5) and recovery (□) experiments on a single patch using 300 nM cisatr on embryonic receptors at −50 mV. The fractional inhibition of nAChR by cisatr was plotted as a function of cisatr exposure or washout time. Each curve was fit (gray line) to a one-exponential function and the reciprocal of the time-constant was used to determine the association and dissociation rate constants.

2-fold higher than that for adult receptors. Although we did not directly measure binding, it was possible to estimate binding affinities because the kinetics of cisatr are rate-limiting in the presence of 300 μM ACh. Cisatr has a 2- to 3-fold higher affinity than atracurium, consistent with the difference in their clinical potencies (Bryson and Faulds,

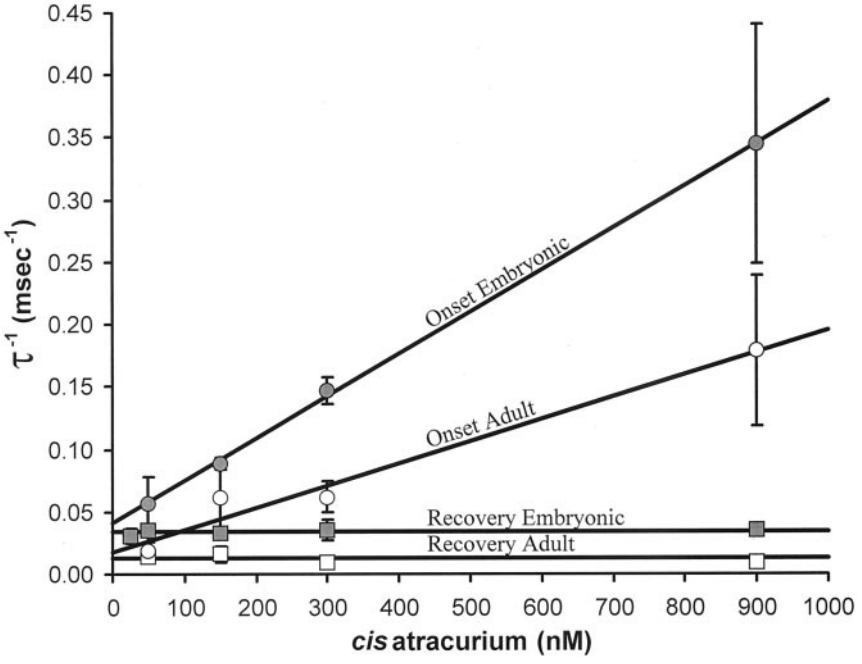

Fig. 7. The reciprocal of the time constant measured from exposure-response curves of onset and recovery protocols in embryonic (solid gray markers) and adult (open markers) receptors at −50 mV plotted as a function of cisatr concentration (three patches per cisatr concentration). The slope of the plot from onset protocols (circles) represents the association rate constant and the ordinate-intercept represents the dissociation rate constant. A more precise estimate of the dissociation rate constant was obtained (average of all points) from the recovery (squares) protocol.

TABLE 2

Results of kinetic experiments obtained from fitting the data in Figs. 5, 6, 7, and 8

The association (ℓ_{+1} Onset) and dissociation (ℓ_{-1} Onset) rate constants in the absence of ACh determined with the onset protocol, dissociation rate constant in the absence of ACh (ℓ_{-1} Recovery) determined with the recovery protocol, the calculated equilibrium constant in the absence of ACh (ℓ_{-1} Recovery/ℓ_{+1} Onset), and the dissociation rate constant in the presence of ACh (ℓ'_{-1} O + OD) determined with the O + OD protocol for cisatr on embryonic and adult receptors are reported as mean ± S.D.; the number of data points are included within parentheses. The last two rows refer to the kinetics of (+)-tubocurarine and pancuronium in the absence of ACh from Wenningmann and Dilger (2001).

nAChR Isoform	Competitive Antagonist	ℓ_{+1} Onset ($\times 10^8$ $M^{-1}s^{-1}$)	ℓ_{-1} Onset (s^{-1})	ℓ_{-1} Recovery (s^{-1})	ℓ_{-1}/ℓ_{+1} Rec./Onset (nM)	ℓ'_{-1} O + OD (s^{-1})
Adult −50 mV	cisatr	1.8 ± 0.3[a] (12)	18.0 ± 14[a] (12)	12.6 ± 4.8[a] (12)	71 ± 29[a]	32.9 ± 5.3[ab] (36)
Embryonic −50 mV	cisatr	3.4 ± 0.3 (12)	40.9 ± 19 (12)	34.2 ± 6.2 (15)	101 ± 22	52.0 ± 9.3[b] (11)
Embryonic +50 mV	cisatr	N.A.	N.A.	30.9 ± 2.3 (5)	N.A.	N.A.
Embryonic −50 mV	(+)-Tubocurarine	1.2 ± 0.2[c] (11)	6.5 ± 2.2[c] (11)	5.9 ± 1.3[c] (8)	50 ± 15[c]	N.A.
Embryonic −50 mV	Pancuronium	2.7 ± 0.9[c] (14)	1.9 ± 1.2[c] (14)	2.1 ± 0.7[c] (12)	7.8 ± 3.7[c]	N.A.

Multiple statistical comparisons were performed within and between rows (see *Results*): [a], $p < 0.003$ for comparison of cisatr kinetics on adult receptors with those on embryonic receptors (−50 mV).

[b], $p < 0.0001$ for comparison of ℓ'_{-1} with ℓ_{-1}.

[c], $p < 0.01$ for comparison of the kinetics of cisatr with those of (+)-tubocurarine and pancuronium on embryonic receptors using one-way analysis of variance Student-Newman-Keuls multiple comparisons test. The values of ℓ_{-1} of cisatr from embryonic receptors were not significantly different at −50 and +50 mV. The values of ℓ_{-1}/ℓ_{+1} of cisatr from adult and embryonic receptors were not significantly different than their corresponding IC_{50} values (Table 1).

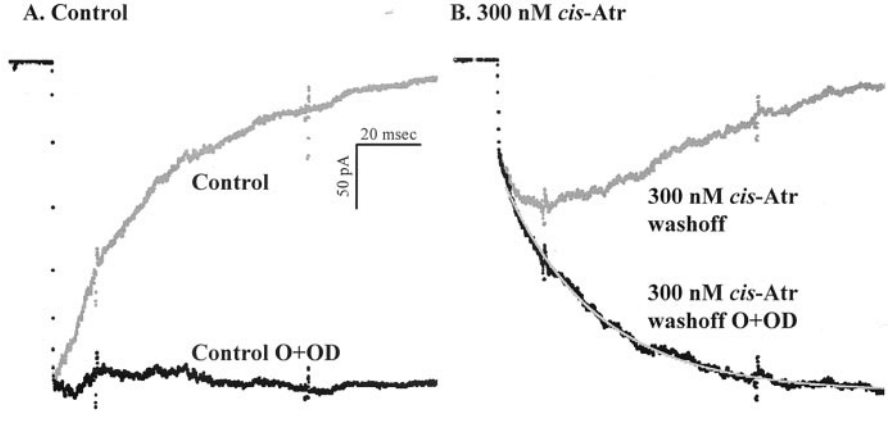

Fig. 8. Results from a representative O + OD protocol using 300 nM cisatr on embryonic nAChR at −50 mV. A, a control current (gray trace) and the corresponding O + OD calculation (black trace), which was a linear horizontal trace (with negligible slope) after the peak rapid onset, suggesting that before desensitizing, most channels are in the open state with 300 μM ACh. B, a 300 nM cisatr washoff current (gray trace). A two-tube perfusion protocol was used to equilibrate the patch with cisatr and then simultaneously (within 200 μs) remove cisatr and activate channels with ACh. The corresponding O + OD calculation (black trace) was fit (superimposed gray trace) to a one-exponential function and the reciprocal of the time constant (20 ms) revealed the dissociation rate constant for cisatr in the presence of ACh.

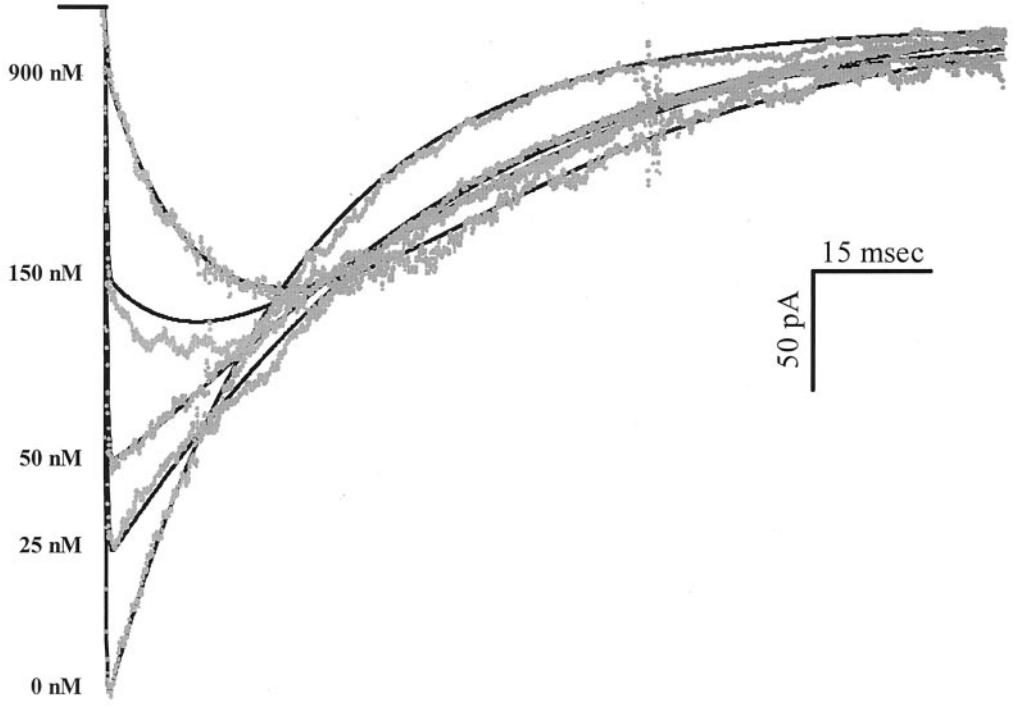

Fig. 9. Comparison between 11-state-model simulation using experimentally-measured mean values (black trace) and drug series (gray trace) from embryonic receptors at −50 mV. The R^2 (eq. 3) between simulated currents and experimental traces for 0, 25, 50, 150, 300, and 900 nM cisatr was 0.998, 0.997, 0.995, 0.986, and 0.984, respectively. The rate constants used for this simulation were (in micromolar^{-1} s^{-1} or s^{-1}): ℓ_{+1} = 340; ℓ_{-1} = 34; ℓ_{+2} = 340; ℓ_{-2} = 1122; ℓ'_{+1} = 440; ℓ'_{-1} = 52; ℓ'_{+2} = 440; ℓ'_{-2} = 1716; k_{+1} = 39; k_{-1} = 1241; k_{+2} = 91; k_{-2} = 5649; β = 27000; α = 376; k_{+D} = 41; and k_{-D} = 0.53.

1997). Cisatr has no appreciable voltage-dependence for competitive inhibition, as reported for (+)-tubocurarine (Colquhoun et al., 1979). In embryonic receptors, there was about a 33-fold difference in affinity between the two binding sites. Consistent with this result, the Hill coefficient of 1.0 suggests that cisatr is interacting primarily with one site (Sine and Taylor, 1981). For adult receptors, there is a difference between the two affinities of ≥8-fold. This is greater than that reported for atracurium but is consistent with the lower Hill coefficient of cisatr compared with that of atracurium (Fletcher and Steinbach, 1996). It was necessary to incorporate the low-affinity site into the 11-state model simulations to accurately simulate experimental traces from adult receptors, but not embryonic receptors, at cisatr concentrations ≥150 nM.

In the equilibrium measurements, ACh was applied to an outside-out patch in the constant presence of cisatr. Cisatr inhibited the initial peak inward currents in a concentration-dependent manner. At low concentrations (<50 nM), the decay time course was similar to that of control. However, at higher concentrations, after the initial rapid activation, the decay exhibited a slow secondary increase in current before desensitizing. A similar, albeit smaller, biphasic behavior was also observed for (+)-tubocurarine (Wenningmann and

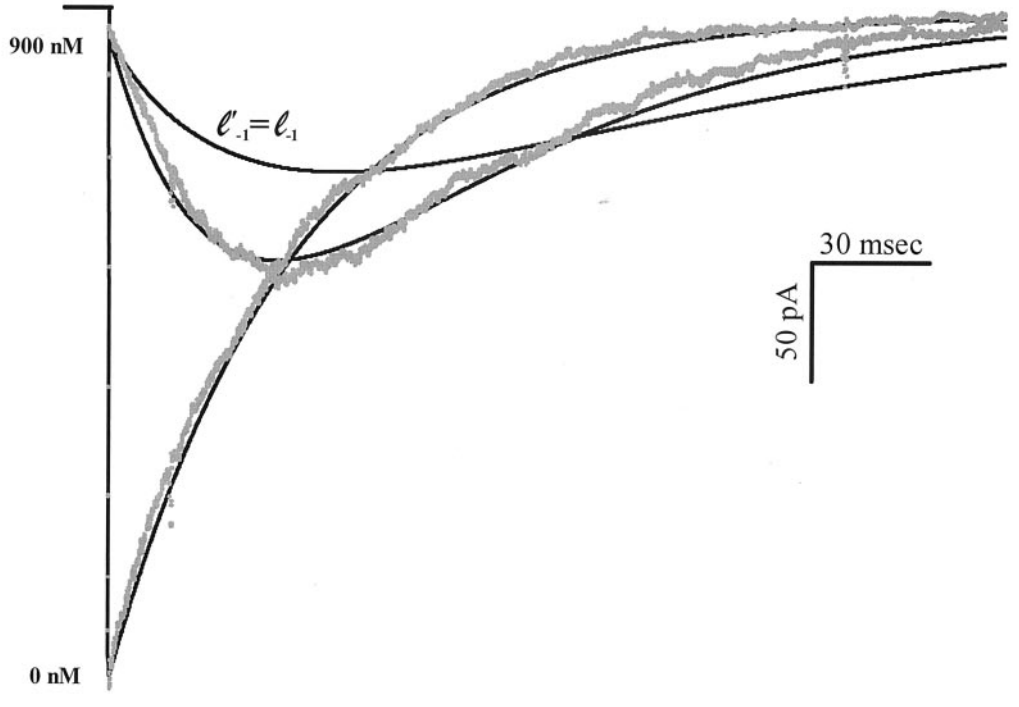

Fig. 10. Comparison between 11-state-model simulation using experimentally-measured mean values (black trace) and drug series using 900 nM cisatr (gray trace) from adult receptors at −50 mV. The simulated current (χ^2 = 1.41; R^2 = 0.974) using distinct rates for ℓ_{-1} and ℓ'_{-1} agreed significantly better ($p < 0.0001$) with the experimental trace than simulated currents (χ^2 = 1845.3; R^2 = 0.598) using the same rate for ℓ_{-1} and ℓ'_{-1}. The rate constants used for this simulation were (in micromolar^{-1} s^{-1} or s^{-1}): ℓ_{+1} = 180; ℓ_{-1} = 12.6; ℓ_{+2} = 180; ℓ_{-2} = 113; ℓ'_{+1} = 429; ℓ'_{-1} = 32.9; ℓ'_{+2} = 429; ℓ'_{-2} = 296; k_{+1} = 220; k_{-1} = 18000; k_{+2} = 110; k_{-2} = 36000; β = 50000; α = 1200; k_{+D} = 26; and k_{-D} = 0.13.

Dilger, 2001). To further investigate this phenomenon, we first considered the possibility that a hetero-liganded open conformation of the channel was being activated. We incorporated the kinetics of this state into our simulations. However, the opening rate was too small to account for the observed currents. Moreover, the biphasic behavior was also present in adult receptors, which do not exhibit hetero-liganded openings (Fletcher and Steinbach, 1996). Our next hypothesis was that cisatr dissociates from the receptors on the millisecond time scale and, as cisatr dissociates, ACh (present at saturating concentrations) binds to the receptors and activates the channels. To test this hypothesis, it was necessary to determine the kinetics of inhibition.

Using the onset and recovery protocols, we determined the association and dissociation rate constants for cisatr. Because ACh is not present during the interval when cisatr is being added or removed, these rates represent transitions between states CR ↔ R in Fig. 2. There is excellent agreement between the antagonist affinity determined from these kinetic experiments (Table 2) and that obtained from equilibrium experiments (Table 1). The association rate is 20-fold greater than that reported for ACh in embryonic receptors (Zhang et al., 1995) and comparable with that reported for ACh in adult receptors (Auerbach and Akk, 1998). Because cisatr is about 10-fold larger than ACh, its high association rate suggests that it may not compete with ACh for the putative agonist-binding site (Miyazawa et al., 1999). Instead, it may bind at or near the tunnel entrance and sterically hinder the entrance of ACh into the tunnel, as suggested by Wenningmann and Dilger (2001). The association rate is probably not diffusion-limited; it is antagonist-specific: cisatr has a significantly larger association rate than pancuronium (1.3-fold) and (+)-tubocurarine (2.9-fold). The association rate of cisatr for embryonic receptors is 2-fold greater than that for adult receptors, suggesting that the ϵ-subunit contributes additional diffusion barriers to cisatr than the γ-subunit.

The dissociation rate of cisatr is markedly higher than that of (+)-tubocurarine (6-fold) and pancuronium (16-fold). The rapid dissociation rate is consistent with our hypothesis: in an equilibrium measurement, cisatr dissociates at a rate faster than or comparable with the rate of desensitization and allows ACh to bind to and activate additional receptors. The excellent agreement between equilibrium measurements and the 11-state model simulation provided a quantitative demonstration that the biphasic time course is caused by antagonist dissociation. Moreover, it helped to establish the accuracy of the rates measured experimentally and provided a quantitative assessment of the contribution (or lack of) for each state and kinetic component. Finally, it demonstrated that an 11-state model is sufficient to describe competitive antagonism of nAChR.

At a synapse, antagonists interact with the receptor both in the presence (CRA 171 RA in Fig. 2) and absence (CR ↔ R) of ACh. Thus, we developed a mathematical technique that removes the effect of desensitization to determine the dissociation rate of an antagonist in the presence of ACh. For both adult and embryonic receptors, we found that the dissociation rate of cisatr in the presence of ACh was significantly larger than that in the absence of ACh. These distinct rates were necessary for the 11-state model simulation to describe accurately the experimental currents (Fig. 10). These findings suggest that the presence of ACh on one site decreases the affinity of cisatr for the other site, at least by increasing its dissociation rate. Consistent with this concept, a study using fluorescence binding assays reported that the binding of ACh or antagonist to one site on *Torpedo californica* nAChR causes a conformational change that alters the affinity of the other site (Covarrubias et al., 1986). More recently, it has been shown the binding of ACh to the receptor causes a "conformational wave" to spread throughout the whole receptor, and a low-to-high affinity change for ACh at the transmitter-binding sites precedes the complete opening of the pore (Grosman et al., 2000). Because single-liganded openings have been observed in embryonic receptors (Sine and Steinbach, 1986; Parzefall et al., 1998), it is plausible that the binding of ACh to a single site causes a global conformation change that alters the affinity of the other site.

There is a large margin of safety (~80%) for competitive antagonism of nAChR at the neuromuscular junction (Paton and Waud, 1967). More than 95% of the receptors are occupied during clinical administration of cisatr. Because cisatr dissociates at a rate of 52/s in the presence of ACh at room temperature, during synaptic transmission (~2 ms), about 10% of the receptors [Free $R = 1 - \exp(-0.002 \times 52)$], may become unoccupied (possibly more at 37°C). In the presence of saturating concentrations of ACh, the kinetics of cisatr is determined by the dissociation rate rather than the association rate (see simulation results). This should reduce the potency of cisatr during synaptic transmission. The direct clinical implications of this are not clear. Monte Carlo simulations are required to provide further insight.

Our results show that cisatr has a markedly higher IC_{50} value than (+)-tubocurarine or pancuronium, primarily because of its high dissociation rate. An antagonist with a higher dissociation rate should have a faster clinical onset time for muscle relaxation because it will equilibrate faster with junctional receptors (Rang, 1974) and its diffusion will be buffered to a lesser extent by extrajunctional receptors (Glavinovic et al., 1993). However, our results are not consistent with clinical observations that cisatr has a significantly slower clinical onset time than pancuronium (1.2-fold) and (+)-tubocurarine (1.7-fold) (Kopman, 1989; Kopman et al., 1999). Moreover, the clinical potency of cisatr is 1.3- and 10-fold greater than that of pancuronium and (+)-tubocurarine, respectively (Savarese et al., 2000). The disparity may be related to temperature. For pancuronium, there was a 2-fold decrease in potency from 29 to 38°C in cats (Miller et al., 1978), in contrast to an increase in potency for (+)-tubocurarine (Ham et al., 1978). In denervated rat hemidiaphragm, there was a 10-fold increase in the apparent binding affinity of (+)-tubocurarine from 22 to 30°C (Banerjee and Ganguly, 1996). However, this finding was obtained using muscle contraction, a very indirect indicator of antagonist activity. Nevertheless, a study using a radiolabeled binding assay on *T. californica* electric organ membranes, reported a 10-fold increase in the binding affinity of (+)-tubocurarine (for open-channel block) from 22 to 37°C (Shaker et al., 1982). To our knowledge, the temperature-dependence of cisatr has not been studied. Studies with other competitive antagonists suggest that they are selectively sensitive to temperature and have varying degrees of responses (Yoneda et al., 1991). Therefore, it is necessary to conduct direct kinetic measure-

ments at 37°C to increase our understanding of the clinical condition.

Acknowledgments

We thank Ms. Claire Mettiwie for help with tissue culture and transfection; Dr. David Colquhoun for insightful suggestions; Drs. Leon Moore and Chris Clausen for advice on statistical analyses; Dr. Cesar Labarca for providing the α, β, and δ cDNA; and Dr. Steven Sine for providing the ϵ cDNA.

References

Amitai G, Herz JM, Bruckstein R, and Luz-Chapman S (1987) The muscarinic antagonists aprophen and benactyzine are noncompetitive inhibitors of the nicotinic acetylcholine receptor. *Mol Pharmacol* **32:**678–685.

Aoshima H, Inoue Y, and Hori K (1992) Inhibition of ionotropic neurotransmitter receptors by antagonists: strategy to estimate the association and the dissociation rate constant of antagonists with very strong affinity to the receptors. *J Biochem (Tokyo)* **112:**495–502.

Arias HR (2000) Localization of agonist and competitive antagonist binding sites on nicotinic acetylcholine receptors. *Neurochem Int* **36:**595–645.

Auerbach A and Akk G (1998) Desensitization of mouse nicotinic acetylcholine receptor channels. A two-gate mechanism. *J Gen Physiol* **112:**181–197.

Banerjee B and Ganguly DK (1996) Thermodynamics of the interaction of d-tubocurarine with nicotinic receptors of mammalian skeletal muscle in vitro. *Eur J Pharmacol* **310:**13–17.

Bryson HM and Faulds D (1997) Cisatracurium besilate. A review of its pharmacology and clinical potential in anaesthetic practice. *Drugs* **53:**848–866.

Bufler J, Wilhelm R, Parnas H, Franke C, and Dudel J (1996) Open channel and competitive block of the embryonic form of the nicotinic receptor of mouse myotubes by D-tubocurarine. *J Physiol (Lond)* **495:**83–95.

Buisson B and Bertrand D (1998) Open-channel blockers at the human $\alpha4\beta2$ neuronal nicotinic acetylcholine receptor. *Mol Pharmacol* **53:**555–563.

Colquhoun D, Dreyer F, and Sheridan RE (1979) The actions of tubocurarine at the frog neuromuscular junction. *J Physiol (Lond)* **293:**247–284.

Colquhoun D and Sheridan RE (1982) The effect of tubocurarine competition on the kinetics of agonist action on the nicotinic receptor. *Br J Pharmacol* **75:**77–86.

Covarrubias M, Prinz H, Meyers HW, and Maelicke A (1986) Equilibrium binding of cholinergic ligands to the membrane-bound acetylcholine receptor. *J Biol Chem* **261:**14955–14964.

Dilger JP (1997) Structure and function of the nicotinic acetylcholine receptor, in *Anesthesia: Biological Foundations* (Yaksh TL ed) pp 221–236, Lippincott-Raven Publishers, Philadelphia.

Dilger JP and Brett RS (1990) Direct measurement of the concentration- and time-dependent open probability of the nicotinic acetylcholine receptor channel. *Biophys J* **57:**723–731.

Fletcher GH, and Steinbach JH (1996) Ability of nondepolarizing neuromuscular blocking drugs to act as partial agonists at fetal and adult mouse muscle nicotinic receptors. *Mol Pharmacol* **49:**938–947.

Glavinovic MI, Law Min JC, Kapural L, Donati F, and Bevan DR (1993) Speed of action of various muscle relaxants at the neuromuscular junction binding vs. buffering hypothesis. *J Pharmacol Exp Ther* **265**:1181–1186.

Grosman C, Zhou M, and Auerbach A (2000) Mapping the conformational wave of acetylcholine receptor channel gating. *Nature (Lond)* **403:**773–776.

Ham J, Miller RD, Benet LZ, Matteo RS, and Roderick LL (1978) Pharmacokinetics and pharmacodynamics of d-tubocurarine during hypothermia in the cat. *Anesthesiology* **49:**324–329.

Hou VY, Hirshman CA, and Emala CW (1998) Neuromuscular relaxants as antagonists for M2 and M3 muscarinic receptors. *Anesthesiology* **88:**744–750.

Kopman AF (1989) Pancuronium, gallamine, and d-tubocurarine compared: is speed of onset inversely related to drug potency? *Anesthesiology* **70:**915–920.

Kopman AF, Klewicka MM, Kopman DJ, and Neuman GG (1999) Molar potency is predictive of the speed of onset of neuromuscular block for agents of intermediate, short, and ultrashort duration. *Anesthesiology* **90:**425–431.

Le Dain AC, Madsen BW, and Edeson RO (1991) Kinetics of D-tubocurarine blockade at the neuromuscular junction. *Br J Pharmacol* **103:**1607–1613.

Miller RD, Agoston S, van der Pol F, Booij LH, Crul JF, and Ham J (1978) Hypothermia and the pharmacokinetics and pharmacodynamics of pancuronium in the cat. *J Pharmacol Exp Ther* **207:**532–538.

Miyazawa A, Fujiyoshi Y, Stowell M, and Unwin N (1999) Nicotinic acetylcholine receptor at 4.6 Å resolution: transverse tunnels in the channel wall. *J Mol Biol* **288:**765–786.

Parzefall F, Wilhelm R, Heckmann M, and Dudel J (1998) Single channel currents at six microsecond resolution elicited by acetylcholine in mouse myoballs. *J Physiol (Lond)* **512:**181–188.

Paton WD, and Waud DR (1967) The margin of safety of neuromuscular transmission. *J Physiol (Lond)* **191:**59–90.

Prince RJ, and Sine SM (1996) Molecular dissection of subunit interfaces in the acetylcholine receptor. Identification of residues that determine agonist selectivity. *J Biol Chem* **271:**25770–25777.

Rang HP (1974) Acetylcholine receptors. *Q Rev Biophys* **7:**283–399.

Savarese JJ, Caldwell JE, Lien CA, and Miller RD (2000) Pharmacology of muscle relaxants and their antagonists, in *Anesthesia* (Miller RD ed) pp 412–490, Churchill Livingstone, Philadelphia.

Schubert D, Harris AJ, Devine CE, and Heinemann S (1974) Characterization of a unique muscle cell line. *J Cell Biol* **61:**398–413.

Shaker N, Eldefrawi AT, Aguayo LG, Warnick JE, Albuquerque EX, and Eldefrawi ME (1982) Interactions of d-tubocurarine with the nicotinic acetylcholine receptor/channel molecule. *J Pharmacol Exp Ther* **220:**172–177.

Sine SM and Steinbach JH (1984) Activation of a nicotinic acetylcholine receptor. *Biophys J* **45:**175–185.

Sine SM and Steinbach JH (1986) Activation of acetylcholine receptors on clonal mammalian BC3H-1 cells by low concentrations of agonist. *J Physiol (Lond)* **373:**129–162.

Sine SM and Taylor P (1981) Relationship between reversible antagonist occupancy and the functional capacity of the acetylcholine receptor. *J Biol Chem* **256:**6692–6699.

Waelbroeck M (1994) Identification of drugs competing with d-tubocurarine for an allosteric site on cardiac muscarinic receptors. *Mol Pharmacol* **46:**685–692.

Wastila WB, Maehr RB, Turner GL, Hill DA, and Savarese JJ (1996) Comparative pharmacology of cisatracurium (51W89), atracurium, and five isomers in cats. *Anesthesiology* **85:**169–177.

Wenningmann I and Dilger JP (2001) The kinetics of inhibition of nicotinic acetylcholine receptors by D-tubocurarine and pancuronium. *Mol Pharmacol* **60:**790–796.

Yoneda I, Okamoto T, Aoki T, and Fukushima K (1991) [The effect of temperature on the action of several neuromuscular blocking agents in vitro]. *Masui* **40:**743–748.

Zar JH (1999) *Biostatistical Analysis*. Prentice Hall, New Jersey.

Zhang Y, Chen J, and Auerbach A (1995) Activation of recombinant mouse acetylcholine receptors by acetylcholine, carbamylcholine and tetramethylammonium. *J Physiol (Lond)* **486:**189–206.

Zhu X, Jiang M, and Birnbaumer L (1998) Receptor-activated Ca2 + influx via human Trp3 stably expressed in human embryonic kidney (HEK)293 cells. Evidence for a non-capacitative Ca^{2+} entry. *J Biol Chem* **273:**133–142.

Address correspondence to: James P. Dilger, Ph.D., Department of Anesthesiology, Health Sciences Center L4, SUNY at Stony Brook, Stony Brook, NY 11794-8282. E-mail: jdilger@epo.som.sunysb.edu